Probing of π conjugation in *trans*-polyacetylene using near-infrared photoluminescence spectroscopy

Phillip W. Carter
Department of Chemistry, University of California, Berkeley, Berkeley, California 94720

John D. Porter
Department of Chemistry, University of California, Berkeley, Berkeley, California 94720
and Lawrence Berkeley Laboratory, Berkeley, California 94720
(Received 8 November 1990)

Near-infrared photoluminescence from undoped *trans*-polyacetylene was attributed to emission from "*cis* defects," structures composed of isolated *cis*-(—CH=CH—) bonds embedded within conjugated *trans*-$(CH)_x$ segments. Spectra were found to be independent of residual transition-metal impurities in the polymer, but quantum efficiencies decreased with increasing concentrations of neutral defects and free carriers. The percolation limit for free carriers was achieved at about 30% overall *trans*-$(CH)_x$. The photoluminescence energy varied inversely with the length of the conjugated *cis* defects, with a different dependence than for polyenes in solution. Interchain interactions were found to be significant in the solid state, distorting bonding geometries and perturbing the electronic structure of the chains; we postulate they are essential for bulk conduction. Hückel calculations yielded $\beta_0 = 1.08$ eV for the π interaction energy, predicting an energy of 0.39–0.43 eV for the π-π^* transition of a typical bound neutral soliton. The band gap for *trans*-polyacetylene of infinite conjugation length was estimated to be 1.20 eV by extrapolation of the solid-state luminescence data. We conclude that thermally isomerized *trans*-polyacetylene is best described as being a three-dimensional ensemble of short, conjugated segments that are bounded and interconnected by defects and crosslinks. Mean segment lengths are probably less than 13 (—CH=CH—) units.

I. INTRODUCTION

Polyacetylene has been the subject of extensive research because of its unique optical and electronic properties and because of the ease of its synthesis. Most previous work idealizes polyacetylene, $(CH)_x$, as a network of infinite, highly conjugated, one-dimensional hydrocarbon chains of isomorphous structure.[1] The ideal isomeric structures for polyacetylene are shown in Fig. 1. For simplicity, the *trans*-transoidal structure is usually referred to as *trans,* and *cis* refers to the *cis*-transoidal structure. Transition-metal-catalyzed synthesis of polyacetylene at low temperatures yields the *cis* isomer. *trans*-polyacetylene is the thermodynamically most stable structure and is obtained irreversibly from *cis*-$(CH)_x$ precursors through thermal isomerization.[2]

Thermally isomerized polyacetylene is usually considered to be composed of extended *trans*-conjugated chains. Typically, the electronic absorption spectrum of isomerized *trans*-polyacetylene is analyzed in terms of data from solvated oligomers, extrapolated using an empirical inverse chain-length dependence.[3] Possible perturbations to the physical and electronic structure of polyacetylene due to the solid-state environment have been largely ignored in the past. Theories concerning conduction mechanisms, optical properties, and observed vibrational modes have been based in large measure upon models appropriate for extended one-dimensional domains of idealized structures located within the polymer network.

If the chemical and physical processes involved in the synthesis of *trans*-polyacetylene are considered in more detail, then it is obvious that there will always be finite concentrations of both *cis* and *trans* subunits in real samples of the polymer. We believe it is vitally important to take into account not only the length, energy, and spatial distributions of various isomeric structures along a single chain, but also their spatial distribution in the ensemble of chains in the solid state. In this paper we reexamine

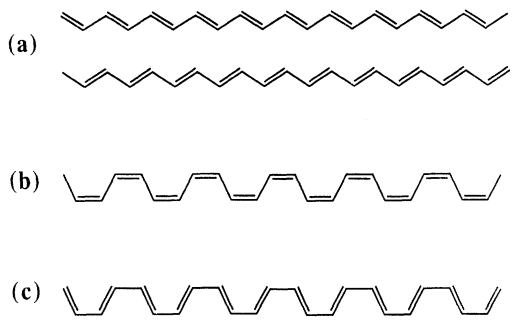

FIG. 1. Ideal structural isomers of polyacetylene. (a) Degenerate conformations of *trans*-transoid, the lowest-energy forms; (b) *cis*-transoid, produced by low-temperature metal-catalyzed polymerizations; (c) *trans*-cisoid.

the relationship between physical and electronic structure in real samples of polyacetylene. From an experimental perspective, we determine the relative importance of intrachain conjugation and of interchain interactions in determining the macroscopic electronic properties of polyacetylene.

The infrared photoluminescence of polyacetylene can be used to study the electronic structure of conjugated chains in the polymer. Low-energy emissions are associated with the lowest π-π^* transition of the polyene chains. Photoluminescence studies have been performed previously,[4] but extremely low emission intensities made it difficult to determine the identities and structures of the luminescent centers. In particular, intrinsic and extrinsic film impurities or chain defects could not be eliminated as possible radiative recombination centers. However, the results of the previous studies tend to support the hypothesis that photoluminescence originates from radiative recombination of excitons bound within individual *trans*-conjugated segments.

In this study we have used a variety of synthetic procedures and we have characterized products using Fourier-transform infrared (FTIR) and resonance Raman spectroscopies and elemental analysis, in addition to performing the photoluminescence experiments. It is our conclusion that the radiative recombination center is an isolated *cis*-(—CH=CH—) bond embedded within a *trans*-conjugated segment. We hypothesize that the *cis* bond serves to pin and localize photogenerated excitons formed on the polyacetylene chain. In our model of *trans*-polyacetylene, the lengths of conjugated segments are limited by defects and crosslinks. As we demonstrate below, experimental photoluminescence spectra can be fit well by model curves calculated on the assumption of limited intrachain conjugation. Hückel calculations also provided support for this description of solid-state polyacetylene as an ensemble of short polyene segments.

II. EXPERIMENT

A. Synthesis

Polyacetylene films and powders were synthesized by polymerizing acetylene gas. Heterogeneous transition-metal catalysts and standard vacuum line techniques were used. Literature preparations were adapted for the use of a series of different transition-metal catalysts. The crude polymers contained different transition-metal impurities bound at the chain ends, depending on the catalyst employed. Table I lists the transition metals used and gives the polymerization conditions. The (Al-to-transition-metal) molar ratio was equal to 4 for all catalysts in the table except for the Ref. 8 catalyst. The solvent used in all polymerizations was dried, distilled, degassed toluene.

Typically, acetylene gas was admitted into the evacuated reaction vessel containing the catalyst solution at an initial pressure of 30–60 kPa, and the formation of the polymer product was usually visible immediately. All products were soaked and washed thoroughly in toluene until no residual catalyst was extracted into solution. Typically, about 0.5–2.5 wt.% transition-metal impurity remained chemically and physically bound in the washed films after the removal of the solvent under vacuum. By maintaining the samples at low temperatures and in an inert atmosphere until this point in the synthesis, it was possible to produce polymers with very low *trans* content, very low neutral defect levels, and very low intrinsic doping levels.

To obtain metal-free polymer samples, the bound transition metal was removed from the chain ends by soaking solvent-swollen films in 10% HCl/CH_3OH for 8 h at $-76\,^{\circ}C$ under a nitrogen atmosphere. This gave films with <0.05 wt.% transition metal after washing with solvent and then removing the solvent under vacuum. After removal of the catalyst and the solvent, the films were stable in normal laboratory air for extended periods (weeks).

An all-*trans*-polyacetylene sample was synthesized using a dilute titanium catalyst solution at 25 °C; the elevated polymerization temperature greatly reduced the *cis*-isomer concentration in the resulting *trans*-rich polymer.

Thermal isomerizations were performed under vacuum, at temperatures ranging from 25 °C to 180 °C in order to obtain the desired *trans*-isomer contents.

B. Photoluminescence and resonance Raman spectroscopy

A bandpass-filtered 5-mW HeNe laser provided 632.8-nm (1.959-eV) excitation, focused to an approximately 200-μm-diam spot on the sample. Average power at the sample was measured to be 2.0 mW using a pyroelectric detector. Sample emission was collected at 180° and collimated. Sharp-cutoff, long-pass filters were used before and after the monochromator to absorb elastically scattered laser light. Cutoff-filter fluorescence was accurately

TABLE I. Polymerization catalysts and reaction conditions.

Catalyst	Reaction Temp. (K)	Reaction time (min)	Major product	Initial % *trans*	Ref.
$Ti(OBu)_4/AlEt_3$	197	2–5	film	6–10	5
$WCl_6/AlEt_3$	197	25	film	10–20	6
$Zr(OBu)_4/AlEt_3$	197	40	film	6–10	
$Y(O\text{-}i\text{-}Pr)_4/AlEt_3$	298	40	powder	20–30	7
$Ti(OBu)_4/AlEt_3$	300	20	colloid	>90	8

measured and was subtracted when greater than 5% of the total signal detected. Emission spectra are uncorrected for spectrometer throughput and quantum efficiency. Typical data-acquisition times were 2–5 h for 1000 points between 650 and 1050 nm. All spectra were recorded with samples free-standing in air at room temperature. No significant spectral changes were observed for most samples over a period of 12 h, implying negligible isomerization, oxidation, or degradation of the samples under irradiation in the spectrometer. Samples studied under dynamic vacuum produced identical photoluminescence spectra to those studied in air.

The mole fractions of *cis*- and *trans*-(—CH = CH—) units in the polymer were determined by FTIR spectroscopy. The intensities of the C-H out-of-plane bending modes[5] at 742 cm^{-1} (*cis*) and 1015 cm^{-1} (*trans*) were used for this purpose. The FTIR data provided no information concerning the spatial organization of the *cis*- and *trans*-(—CH = CH—) units in the polymer, merely their relative abundance. Resonance Raman bands which appear on the luminescence envelope are in agreement with previously reported assignments.[9] The fundamental Raman bands observed in our spectral window are Stokes shifted by 1065 cm^{-1} (*trans*), 1250 cm^{-1} (*cis*), 1460 cm^{-1} (*trans*), and 1540 cm^{-1} (*cis*) from the HeNe excitation line (15 803 cm^{-1}). We did not observe the 910-cm^{-1} *cis* band because of the cutoff filters used in our spectrometer. Emission intensities were reduced due to cutoff-filter

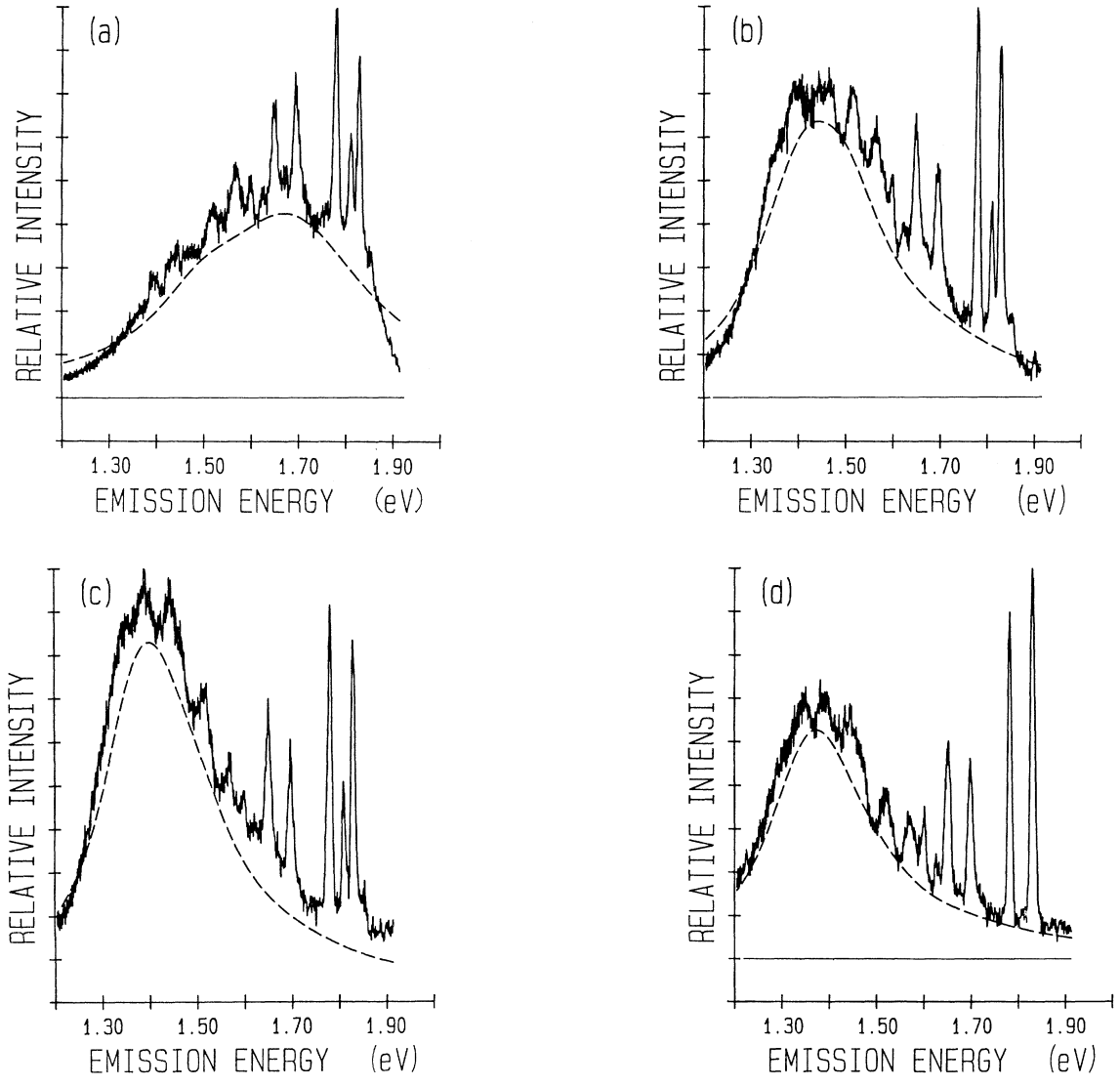

FIG. 2. Photoluminescence spectra of thermally isomerized Shirakawa (titanium catalyst) polyacetylene films. The excitation energy was 1.959 eV (632.8 nm). The sharp features are resonance Raman bands. The broad luminescence envelopes have been fitted by model curves (dashed lines) composed of a sum of Lorentzians, as described in the text. Mole fraction *trans*-$(CH)_x$ content determined by FTIR spectroscopy was (a) 7%, (b) 20%, (c) 54%, and (d) 80%.

absorption at energies greater than 1.8 eV, and this gives rise to the observed asymmetry in the spectra of *cis*-rich polymers. The 1460- and 1540-cm^{-1} Raman bands were usually unresolved at the slit widths used here (4-nm resolution). Overtone Raman bands observed in the emission spectra are mostly linear combinations of the *trans* fundamentals. The intensities of the resonance Raman bands varied with isomer content in a nonlinear fashion that was calibrated using the FTIR data.

III. RESULTS

We observed a photoluminescence emission maximum for as-prepared, >90% *cis*-$(CH)_x$ at 1.68 eV. The emission maximum was redshifted to 1.36 eV upon thermal isomerization to 40% *trans*-$(CH)_x$. Further increase of *trans* content simply decreased the intensity of the 1.36-eV feature. At >90% *trans*-$(CH)_x$, the luminescence signal became very weak but remained detectable. Figures 2(a)–2(d) are photoluminescence spectra for thermally isomerized films of Shirakawa polyacetylene.

The broad polyacetylene photoluminescence feature was found to be *independent* of the catalyst used to prepare the polymers, namely $Ti(OBu)_4/AlEt_3$, $Zr(OBu)_4/AlEt_3$, $WCl_6/AlEt_3$, or $Y(O\text{-}i\text{-}Pr)_3/AlEt_3$, where OBu is butoxy, Et is ethyl, and O-*i*-Pr is isopropoxy. No luminescence features attributable to the metals were observed. For example, Fig. 3 shows photoluminescence spectra for tungsten-catalyzed polyacetylene at two different isomer contents. The *cis-trans* isomer ratios of the purified polymerization products did vary with the catalyst and with reaction conditions, but at equivalent isomer contents the polymer emission spectra were very similar, despite the presence of different residual transition-metal impurities on chain ends. As indicated in Table I, the polymers exhibited a variety of gross physical morphologies. However, photoluminescence spectra of the films, colloids, and powders were not significantly different at similar isomer contents.

Treatment of films with HCl/CH_3OH as described above removed the residual transition metal bound to the chain ends. FTIR and resonance Raman data indicate that this procedure resulted in partial isomerization and introduced a small concentration of free carriers in the polymer. After removal of residual metal, the emission maximum was redshifted, exhibiting a lower intensity relative to the untreated films. The lower emission energy is a result of the catalyzed isomerization.[10] Both transition-metal-catalyzed isomerization and thermal isomerization produced polymers with similar peak emission energies at comparable isomer contents. The presence of free carriers in the metal-free samples, easily seen in the FTIR spectra, decreased radiative recombination efficiency through minority-carrier quenching.

The *trans* samples prepared by thermal isomerization from the *cis*-synthetic precursors always retained some *cis* content as measured by FTIR spectroscopy and some photoluminescence. In contrast, all-*trans*-$(CH)_x$ powders prepared at higher polymerization temperatures exhibited no detectable photoluminescence features in the near infrared even at low free-carrier concentrations. Figure 4 illustrates the featureless spectrum obtained for *trans*-polyacetylene prepared using the high-temperature syn-

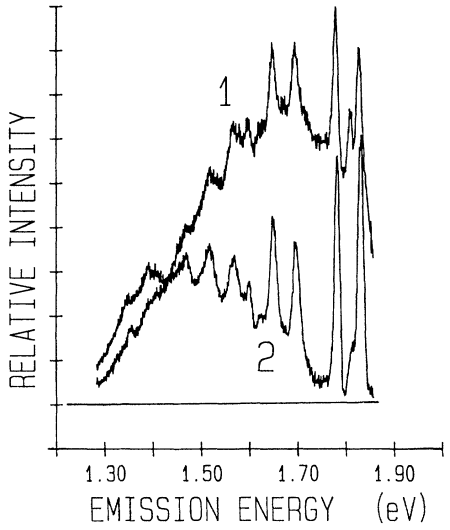

FIG. 3. Photoluminescence spectra of polyacetylene prepared using a tungsten hexachloride-triethyl aluminum catalyst. The excitation energy was 1.959 eV. The resonance Raman bands are identical to Shirakawa polyacetylene. No new luminescence features attributable to tungsten are observed. Mole fraction *trans*-$(CH)_x$ content determined by FTIR spectroscopy was (1) 20%, (2) 70%.

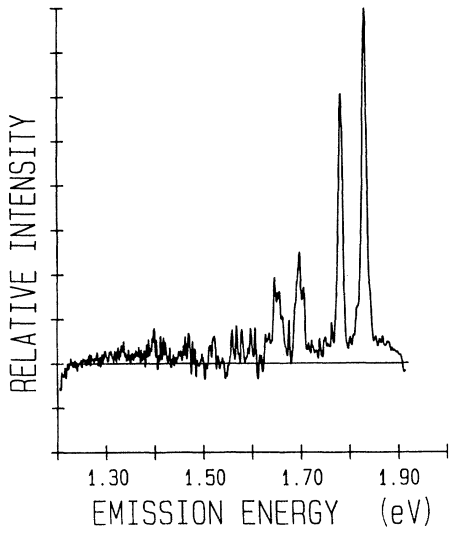

FIG. 4. Photoluminescence spectra of 95% *trans*-polyacetylene prepared by the high-temperature route described in Ref. 8. Excitation energy was 1.959 eV. No detectable luminescence feature was observed and only *trans* resonance Raman bands were present.

thetic route. *trans*-$(CH)_x$ resonance Raman features are prominent, confirming that free-carrier concentrations were very low, but the photoluminescence feature near 1.36 eV is absent.

All of the results presented above indicated that the presence of *cis*-(—CH=CH—) units was necessary in order to observe the infrared photoluminescence. In addition, the polymer photoluminescence spectra were sensitive to relative *cis-trans* isomer content, but they were independent of both the type of transition-metal impurities present at chain ends and the macroscopic physical morphology of the polymers.

IV. DISCUSSION

A. Emission spectroscopy

The near-infrared emission observed in polyacetylene has been attributed to radiative recombination of an exciton bound in a *trans* segment of the polymer. However, consistent with the observations described above, we postulate that radiative recombination takes place at *cis*-(—CH=CH—) bonds embedded within *trans*-conjugated segments of the polymer. The complete structure composed of a *cis* bond plus its associated region of *trans* conjugation will also be referred to as a "*cis* defect." It is well known from previous studies that "pure" *cis*-$(CH)_x$ polyacetylene has a radiative recombination efficiency an order of magnitude higher than "pure" *trans*-$(CH)_x$ (Ref. 11). This difference in quantum efficiency has been attributed to an unfavorable excited-state relaxation pathway involving charge separation in pure *cis*-$(CH)_x$. The nondegenerate ground-state configurations for pure *cis*-polyacetylene result in an energy barrier to charge separation and tend to localize excitons on a single *cis* bond. For pure *trans*-polyacetylene, the formation of a delocalized carbocation-carbanion pair, often termed charged solitons in the literature, is a very rapid and efficient process; the degenerate nature of the all-*trans*-$(CH)_x$ structure means that only a small activation barrier is needed to induce charge separation in the excited state. For solid-state polyacetylene, excitation at a pure *cis* structure results in a localized excited state and a higher quantum efficiency for radiative recombination, whereas at a pure *trans* segment, facile exciton dissociation and migration results in a much higher rate of nonradiative relaxation and a smaller quantum efficiency for photon emission.

The ground-state electronic structure of a "*cis* defect" is expected to lie somewhere between the structures of the pure *cis* and the pure *trans* isomers. Because the $C(2p_z)$ orbitals of the *cis* carbons are mismatched physically and energetically with the surrounding *trans* π system, wave-function overlap in the ground state will be reduced somewhat at the *cis* bond. This will result in a weakening of the Peierls distortion, which leads to bond alternation in the polymer, creating a local energy maximum in the ground-state π system at the *cis*-carbon-carbon bond. In particular, this type of ground-state structural and electronic "defect" in the π chain should act as a trap for mobile, photogenerated holes, since removal of electron density at the *cis* bond will have a minimum effect on the lower-energy *trans* π system that surrounds it.

On the other hand, this same type of *cis* bond is expected to be stabilized in the excited state relative to an all-*cis* segment. The repulsion of spatially proximate hydrogen atoms, associated with π bond elongation in the excited state, is eliminated for the *cis* bonds in the "defect" compared to pure *cis*-$(CH)_x$. Hence, based on steric arguments, the "*cis* defect" is expected to have a smaller π-π^* energy gap relative to an all-*cis* structure. From both the dependence of photoemission on *cis* structure and from steric considerations, it seems likely that a *cis* defect can serve to trap and localize excitons. Exciton trapping at structural defects is common in polymer photophysics.[12] The smaller π-π^* gap on the "*cis* defect" should be reflected in photoemission energies being redshifted relative to pure *cis* photoluminescence. The relevant length scales and efficiencies of exciton trapping at *cis* defects in polyacetylene will be discussed in a section below, using traditional energy-transfer models.

The polyacetylene photoluminescence spectra are modeled in this paper as the sum of emissions arising from a distribution of *cis* defects with different energies. We propose that the defect energies are primarily dependent on both the nature of conjugation within the defect structure and on the degree of interchain interactions. Wegner has previously discussed the presence of interchain interactions in polyacetylene.[13] It must be emphasized that most real polyacetylene samples have significant interchain interactions due to the crosslinking reactions that are prevalent for extended polyenes.[14]

Interchain C—C bond formation forces neighboring π systems into unusually close proximity. Unlike many other solid-state π systems, polyacetylene chains are not packed together by van der Waals forces alone. The reactive π system in polyacetylene is a sterically unprotected hydrocarbon chain, making it uniquely susceptible to extensive thermal and photochemical crosslinking reactions. Crosslinking serves to shorten average interchain distances from their van der Waals equilibrium values. Studies of other π systems with limited conjugation have shown that increased π overlap in the solid state results in reduced π-π^* radiative recombination energies and greater tendency towards dissociation of photogenerated excimers.[15] Well-characterized, short, soluble polyacetylene derivatives have been found to have absorption spectra which are redshifted in the solid state compared to their spectra in solution.[16] Clearly, interchain perturbations play a significant role in reducing the π-π^* energy difference in solid-state polyacetylene. With the presence of significant perturbations to π-π^* energetics due to π stacking, it is not necessary to invoke a model of infinite one-dimensional polyene conjugation in order to explain the low π-π^* energy differences observed in this material.

B. Modeling

To model polyacetylene in terms of localized conjugation, we have considered the polymer to be constructed of

an assembly of interacting "*cis* defect" units, possibly bound in close proximity by sp^3 carbons, and separated along a given polymer chain by stretches of pure *cis*-$(CH)_x$ and sp^3 carbons. We have chosen structures in which the addition of *trans* units takes place in pairs, since this is consistent with a plausible thermal isomerization mechanism.[10] As a first approximation, the *cis* defects are modeled as $(trans)_m$-*cis*-$(trans)_m$, where m is the number of pairs of *trans* units in the defect. Each value of m corresponds to a local structure possessing unique trap energetics. The highest energy trap in our model corresponds to structures where $m=1$; the highest observed peak emission at 1.68 eV was assigned to this highest-energy trap. Each increase in the number of pairs of *trans* segments corresponds to a lower trap energy. Therefore, the photoluminescence spectra are predicted to depend upon *cis-trans*-isomer ratios in a way which is different from FTIR spectra. The total conjugation length of a *cis* defect is represented by n, where $n=2(m)+1$.

The experimental luminescence envelopes were fitted by a sum of Lorentzian curves. Model curves composed of such sums are shown as dashed lines in Fig. 2. The Lorentzian parameters were chosen by inspection, by analyzing complete series of spectra recorded during thermal isomerization of polyacetylene samples. The minimal set of model Lorentzians necessary to fit all observed luminescence spectra were determined in this way. Table II lists the hypothesized structures and their Lorentzian spectral parameters. We found that all polyacetylene photoluminescence curves could be fitted by linear combinations of model curves defined for $m=1$, 2, 3, 4, 5, and 6, i.e., for $n=3$, 5, 7, 9, 11, and 13.

Figure 5 shows the empirical linear relationship between reciprocal *cis*-defect conjugation length $(1/n)$ obtained from the model and the best-fit *cis*-defect energy. There is a strong linear correlation that is typical for conjugated polyene models. The extrapolated π-π^* energy gap of 1.20 eV at infinite conjugation is appropriate for a single *cis* defect in the solid state, and is a good approximation to the band gap of pure *trans*-$(CH)_x$. The slope of Fig. 5 reveals a much smaller dependence of π energetics on conjugation length than for polyenes in solution. We postulate that the smaller intrachain conjugation is the result of distorted chain geometries being "locked" into the solid-state structures, disrupting "pure" sp^2 hybridization significantly. The crosslink defects and the resulting forced interchain proximity are not present for "free" polyene molecules in solution, and inhomogeneities in local environments are less extreme in solution compared to the solid state. For this reason, we believe that the common practice of directly applying solution-phase data to models of solid-state π conjugation may not be appropriate. The trend in observed best-fit half-widths of the model curves are consistent with larger perturbations on π energetics for the shorter conjugation lengths.

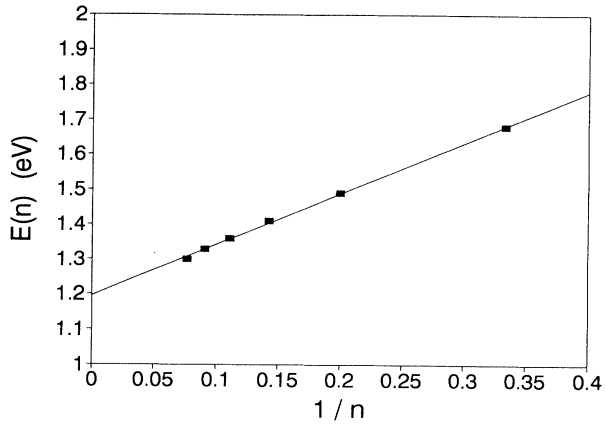

FIG. 5. Plot of the best-fit "*cis*-defect" emission energies $E(n)$ as an empirical function of the reciprocal conjugation length of the defect, $(1/n)$, where n is the total number of *cis*- and *trans*-(—CH=CH—) units in the defect. The empirical best-fit regression line has the formula $[E(n)/\text{eV}] = 1.196 + (1.461/n)$.

TABLE II. Lorentzian parameters used for fitting photoluminescence spectra.

"*cis*-defect" structure	Maximum (eV)	Half-width (eV)
-$(trans)_1$-*cis*-$(trans)_1$-	1.68	0.40
-$(trans)_2$-*cis*-$(trans)_2$-	1.49	0.24
-$(trans)_3$-*cis*-$(trans)_3$-	1.41	0.18
-$(trans)_4$-*cis*-$(trans)_4$-	1.36	0.17
-$(trans)_5$-*cis*-$(trans)_5$-	1.33	0.16
-$(trans)_6$-*cis*-$(trans)_6$-	1.30	0.16

Radiative recombination kinetics were assumed to be approximately the same for all the *cis*-defect structures, which is reasonable if the lone *cis*-(—CH=CH—) bond in the defects is the recombination site, as argued above. Therefore, provided that the luminescence centers were randomly distributed in a uniform matrix, competition between radiative and nonradiative relaxation pathways was a constant for all defects at any given polymer composition, even if nonradiative recombination varied with polymer composition. Hence, the distributions of *cis*-defect structures in the polymer could be calculated by fitting the observed luminescence spectra.

Figure 6 presents typical histograms obtained from spectral fitting. The normalized fraction of each type of *cis* defect, $f_d(n)$, is plotted as a function of the conjugation length of the defect n for four films of different overall *trans*-(—CH=CH—) mole fraction X_t as determined by FTIR spectroscopy. The evolution of the histograms upon thermal isomerization indicated that the mechanism of isomerization was more like random conversion of *cis* units rather than nucleation and growth of pure *trans* domains. This is consistent with approximately first-order initial kinetics for overall conversion of *cis* to *trans* observed previously.[17] As expected, the trend is to a higher mean value of n, $\langle n \rangle$, as isomerization proceeds. However, it is remarkable that $\langle n \rangle$ remains so low and the distribution remains so broad up to very high overall mole fractions of *trans*-$(CH)_x$. For example,

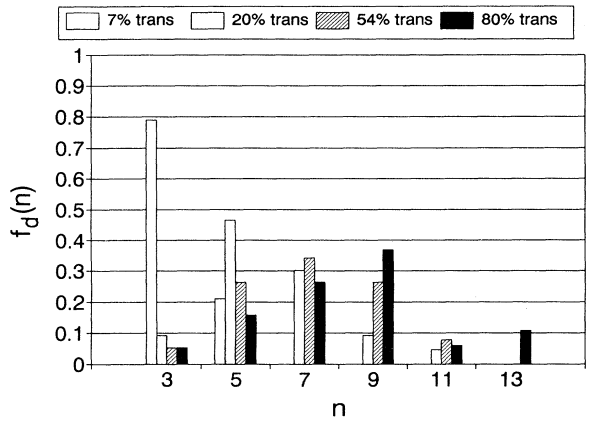

FIG. 6. Histogram of luminescent *cis*-defect populations in thermally isomerized polyacetylene. The fraction of defects with conjunction length n, $f_d(n)$, is plotted as a function of n for four samples of different *trans* mole fractions, as determined by FTIR spectroscopy.

$\langle n \rangle = 8.2$ for the 80% *trans*-$(CH)_x$ sample, $X_t = 0.80$, in Fig. 6. The structural picture of polyacetylene that emerges from the photoluminescence spectra is clearly one of an array of short conjugated segments.

Overall mole fractions of *cis*- and *trans*-(—CH = CH— bonds, X_c and X_t, respectively, were calculated for thermally isomerized polyacetylene samples from the FTIR spectra. The FTIR data provided no information about the physical organization of the *cis* and *trans* units in the polymers, but the spectra did account for all material, including the fraction of the polymers not probed by photoluminescence. For example, photoluminescence from pure *cis*-$(CH)_x$ was not observed experimentally because it occurs at energies too close to our exciting laser, and pure *trans*-$(CH)_x$ is apparently not photoluminescent, according to the results of our experiments.

In the initial stages of isomerization, it is reasonable to assume that the amount of *trans* isomer calculated from the luminescence data is correlated with the total mole fraction of *trans* bonds calculated from the FTIR data, since the presence of a single *cis* bond anywhere within a *trans* segment makes that segment addressable by the photoluminescence experiments. This allowed the two types of spectroscopic data to be combined to give the fraction of the polymer that was composed of luminescent "*cis* defects."

The weighted mean fractions of *cis*- and *trans*-(—CH = CH—) units within the luminescent *cis* defects, $\langle f_{lc} \rangle$ and $\langle f_{lt} \rangle$, respectively, were calculated from weighted sums of the photoluminescence histogram data, taking into account the dependence of *cis* and *trans* content of the defects with n:

$$\langle f_{lc} \rangle = \sum_{n=3}^{\infty} f_d(n) \left[\frac{1}{n} \right], \tag{1}$$

$$\langle f_{lt} \rangle = \sum_{n=3}^{\infty} f_d(n) \left[\frac{(n-1)}{n} \right]. \tag{2}$$

Then, assuming that all of the *trans*-$(CH)_x$ in the sample was contained in the luminescent defects, the mole fraction of the polymer composed of luminescent *cis* defects, X_d, was calculated:

$$X_d = X_t / \langle f_{lt} \rangle . \tag{3}$$

Similarly, the mole fraction of the polymer composed of the radiative recombination sites X_r, i.e., just the luminescent *cis* bonds within the *cis* defects, was calculated:

$$X_r = \langle f_{lc} \rangle X_d . \tag{4}$$

Data were plotted in Fig. 7 as X_d and X_r, two quantities calculated from the photoluminescence data, versus X_t, the mole fraction of *trans* bonds calculated from the FTIR data. The hypothesis that all *trans* units can be addressed by photoluminescence must break down as $X_t \to 1$ under ideal isomerization conditions, since ideal one-dimensional polymers all pass through the point (1,0). In practice, however, the shape of X_d versus X_t curves will depend upon the isomerization mechanism, the effective dimensionality of the material, and the degree of electronic communication between luminescent defects and nonluminescent chromophores. The trends we observed at low X_t were found to continue to overall *trans* fractions as high as $X_t = 0.8$. Again, this was a strong indication that thermal isomerization proceeded according to a mechanism of random conversion, and that polyacetylene was accurately described as a collection of short conjugated segments during isomerization. It is interesting to note that the fraction of radiative recombination sites in the polymer remained small,

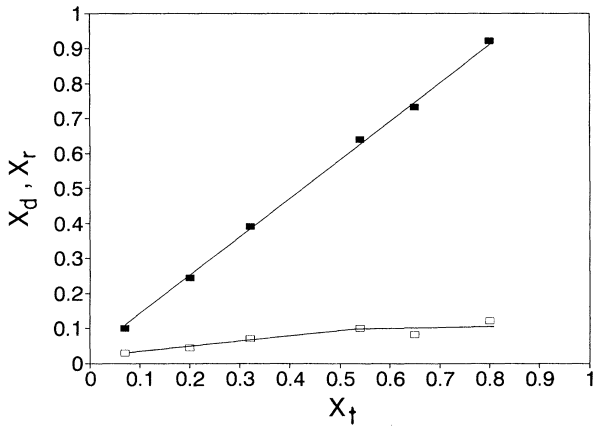

FIG. 7. (■) The mole fraction of (—CH = CH—) units contained in "*cis* defects," X_d, is plotted against the overall mole fraction of *trans*-$(CH)_x$ in thermally isomerized polyacetylene, X_t, as determined by FTIR spectroscopy. The regression line extrapolates to $X_d = 1$ at $X_t = 0.88$. (□) The mole fraction of photoluminescent *cis*-(—CH = CH—) bonds X_r is plotted against the overall mole fraction of *trans*-$(CH)_x$ in thermally isomerized polyacetylene, X_t, as determined by FTIR spectroscopy. Above $X_t = 0.3$, X_r remains roughly constant near $X_r = 0.1$.

around $X_r = 0.1$, and nearly constant between $X_t = 0.3$ and 0.8.

By extrapolation, the data in Fig. 7 indicate that $X_d \rightarrow 1$ in thermally isomerized polyacetylene at an overall composition of 12% *cis* and 88% *trans*. The mean conjugation length of the *cis* defects at that point would be $\langle n \rangle = (X_t / X_c) = 7.3$, which is close to the mean of the distribution shown in Fig. 6 for the 80% *trans* sample, $\langle n \rangle = 8.2$. Further increase in the *trans* content above about 80% or so can only be achieved by annealing the polymer at high temperatures for extended periods of time. Under these conditions, it is likely that further increase in the *trans-cis* ratio is achieved not only by converting *cis* to *trans*, and thereby increasing the mean conjugation length, but by chemically reacting and removing *cis* bonds through rearrangements or crosslinking reactions. For instance, if the processes of isomerization and crosslinking were equally probable, then the limiting value of $\langle n \rangle$ in fully isomerized polyacetylene would be just 13, according to our data. All of the luminescence spectra could be fitted by summing emissions from structures corresponding to $n = 13$ or less.

C. Hückel molecular-orbital calculations

Hückel theory has been extremely successful in developing useful correlations between the length of conjugated polyenes and their electronic absorption spectra in solution.[18] Here we have applied similar calculations to short polyenes in the solid state. In the present polyene calculations, only π orbitals involved in chain conjugation were considered. π-π^* highest occupied molecular orbital, lowest unoccupied molecular orbital energy differences were computed for several values of β_0, the interaction energy between adjacent π orbitals. In the past, Hückel calculations of conjugated polyenes have been performed using a single effective value for β_0 and a single carbon-carbon bond length.[19] We included bond alternation in the present calculations by using different overlaps to describe "single" and "double" bonds. The variation of β_0 with carbon-carbon bond length has been approximated previously, with unit β_0 corresponding to a carbon-carbon distance of 1.397 Å.[20] Undoped polyacetylene linkages were modeled here by C—C and C=C distances of 1.48 and 1.33 Å, corresponding to relative overlaps of $1.23\beta_0$ and $0.67\beta_0$, respectively. Although the best-fit bond alternation used in this study was more exaggerated than experimental evidence suggests,[21] a good fit with the luminescence data was obtained. Our calculations for "defect energies" were made for odd conjugation lengths of 3–13 C=C bonds in total (i.e., $N = 3-13$), having a single *cis* bond in the middle of two equal *trans* segments. The model defects were considered to have C_{2V} symmetry with the π-π^* transition equivalent to a $B_1 \leftarrow A_2$ transition, according to group-theory notation.

Hückel theory does not differentiate between *cis*- and *trans*-C=C bond conjugation, and therefore predicts identical π-π^* energies for -(*trans*)$_{11}$- or -(*trans*)$_5$-*cis*-(*trans*)$_5$- structures. Both of these structures would be represented by $n = 11$ in Hückel theory, since n is equal to the sum of *cis* and *trans* double bonds. However, as we discussed above, the *cis*-C=C bond is believed to act as a trap for excitons, and therefore is the structure that we correlate with radiative recombination at "*cis* defects" in polyacetylene.

The Hückel calculations agreed with the photoluminescence data when $\beta_0 = 1.08$ eV, and the results are shown in Table III. The best-fit β_0 for polyacetylene luminescent defects is significantly lower than for polyenes in solution. This lowering in the mean interaction energy is consistent with significant deviation on average from ideal sp^2 hybridization at the carbon atoms of the polymer. This could be due to distortion of the polymer out of the plane of conjugation in the solid state. Theoretical models for the effects of the dihedral angle on β_0 have been proposed, but were not included in the present treatment. Interchain π stacking would also modify the effects of intrachain conjugation by introducing local changes in π symmetry and electron densities. The agreement between the polyacetylene emission data and this simple Hückel treatment supports a model of short *trans* conjugation in solid-state polyacetylene.

As stated above, bond alternation is often ignored in Hückel calculations, and a single bond length and single effective β_0 are used to describe all carbon-carbon interaction energies. In polyacetylene, this is the structure of fully delocalized states, or solitons, in which bond alternation is lost along the polyacetylene chain.[22] Soliton states can be generated in polyacetylene either photophysically or through chain oxidation or reduction. This approximation results in a simplified expression for the energies of π-π^* transitions in neutral solitons:[18,23]

$$E_s = 4\beta \sin\{\pi/[2(2n+1)]\} \ . \tag{5}$$

Using the appropriate experimental value of $\beta(1.397\ \text{Å}) = 1.08$ eV for polyacetylene in Eq. (5), the hy-

TABLE III. Hückel π-π^* energies calculated using $\beta_0 = 1.08$ eV.

Model	n	Experimental maximum (eV)	*cis* defect (calc) (eV)	Neutral soliton (calc) E_s (eV)
-(*trans*)$_1$-*cis*-(*trans*)$_1$-	3	1.68	1.75	0.96
-(*trans*)$_2$-*cis*-(*trans*)$_2$-	5	1.49	1.50	0.61
-(*trans*)$_3$-*cis*-(*trans*)$_3$-	7	1.41	1.40	0.45
-(*trans*)$_4$-*cis*-(*trans*)$_4$-	9	1.36	1.34	0.36
-(*trans*)$_5$-*cis*-(*trans*)$_5$-	11	1.33	1.31	0.29
-(*trans*)$_6$-*cis*-(*trans*)$_6$-	13	1.31	1.29	0.25

pothetical π-π^* energies for neutral soliton states bound at *cis* defects were calculated for the various conjugation lengths observed experimentally (Table III). For polyacetylene *cis* defects with mean conjugation lengths between $n=7.3$ and 8.2, typical values for 80–90% *trans*-polyacetylene, the π-π^* energy difference is 0.39–0.43 eV. This is close to the 0.45-eV absorption energy observed experimentally, which would correspond to just $\langle n \rangle = 7$, according to our calculations. The delocalization length of a soliton on a *trans*-polyacetylene chain is believed to have an upper limit of 30 carbons (Ref. 24) ($n=15$), which is consistent with the upper bound for the *cis*-defect domains proposed here for thermally isomerized polyacetylene. Our Hückel calculations indicate that, to a first approximation, the π system of thermally isomerized polyacetylene can be treated as an ensemble of rather short polyenes, perhaps as short as 7–9 (—CH=CH—) units on average, and that this model is not in disagreement with observations of solitons in polyacetylene.

D. Exciton trapping efficiency

Although radiative recombination kinetics are not expected to be a function of *cis*-defect length, quantum efficiencies might be expected to be inversely related to the length of the conjugated *cis* defects. This is because exciton trapping and annihilation should be more efficient on defects that are too small to allow facile exciton migration or dissociation away from trap sites. However, we argue above that polyacetylene is composed of *cis* defects that are all equal to or smaller than the size of a delocalized exciton in this material. Hence, as long as generation and recombination take place on the same defect, the kinetics of radiative annihilation of bound excitons would probably be very similar for the different *cis* defects encountered in polyacetylene.

However, generation and annihilation need not take place on the same defect. The relative efficiencies with which excitons are trapped depend strongly upon the distances of the traps from the location of exciton formation. Energy transfer over longer distances (15–60 Å) occurs primarily through dipole-dipole interactions.[25] π excited-state lifetimes are typically in the range 1–100 ns for molecules in solution,[26] and long-range energy migration is common in this case. However, the excited-state lifetime in *trans*-polyacetylene is short, less than 2 ps,[27] and this means that exciton migration or energy transfer is restricted to very short distances in this material. Given the short time scales and the relatively localized character of the bound excitons in this material, dipole-dipole interactions are not expected to be dominant in polyacetylene.

For energy-transfer processes occurring over distances less than about 15 Å, an electron exchange mechanism requiring overlap of electronic states is favored.[28] With these considerations in mind, photoexcitations in polyacetylene occurring at distances greater than 15 Å from a trap site are expected to have poor radiative recombination efficiencies because of the lack of required wave-function overlap. Similarly, exciton migration from trap sites will be restricted to short distances.

Integrated luminescence intensities were found to increase initially with X_t, the overall mole fraction of *trans* bonds, as might be expected from the X_t data in Fig. 7. However, intensities reached a maximum at about $X_t=0.3$, or a mole fraction of *cis* defects $X_d=0.35$. Above this value of X_t, intensities declined steadily, despite the fact that the mole fraction of radiative recombination sites X_r remained approximately constant. The intensity maximum occurred near the percolation threshold for a random, *three*-dimensional composite material. Above this volume fraction of defect structures, free carriers generated during thermal isomerization apparently gained access to trapped excitons, and nonradiative exciton annihilation pathways increased. Also, more extensive exciton migration via nearest-neighbor *cis* defects becomes possible above the percolation threshold, increasing exciton access to thermally generated neutral defects.[29] The dependence of the integrated intensity data upon *trans* content served to further emphasize the difference between real samples of polyacetylene, which behaved like three-dimensional composite materials, and the ideal models of polyacetylene, which emphasize the one-dimensional character of the ideal linear polyene.

The independence of the photoluminescence spectra with transition metals bound at chain ends was consistent with the recombination kinetics and the probable exciton diffusion lengths discussed above. We estimate from elemental analysis and IR spectroscopy that *cis* traps within the defects were about 20 times more concentrated in the samples than metal impurities on chain ends for 90% *trans*-polyacetylene. In addition, a *cis* defect probably has much better overlap physically and energetically with an exciton wave function than does the transition metal at the chain end. Based on these considerations and the poor *cis* trapping efficiency, the transition metal was not expected to affect excited-state relaxation and recombination rates significantly, as observed.

V. SUMMARY

This paper describes polyacetylene as a collection of short, conjugated segments separated along a polymer chain by sp^3 and other defects and packed closely together in the solid state through chain crosslinking. Thermal isomerization of all-*cis*-polyacetylene resulted in the formation of short segments of *trans*-polyacetylene, within which were embedded isolated *cis*(—CH=CH—) bonds. This assembly was referred to as a "*cis* defect." Photogenerated excitons that were generated at or near *cis* defects could become trapped at the *cis*-(—CH=CH—) bond and undergo radiative recombination. The observed photoluminescence emission energies were a function of the conjugation length of the *cis* defect and the extent of local interchain π stacking. Analysis of integrated luminescence intensities indicated that the percolation threshold for free carriers was achieved at just 30% overall *trans* content, implying that thermally isomerized polyacetylene behaved more like a *three*-dimensional composite material than a *one*-dimensional material. At approximately 88% *trans*-$(CH)_x$ content, a

thermally isomerized sample of polyacetylene became equivalent to a sample of "pure" *cis* defect, with the mean conjugation length being just $\langle n \rangle = 7.3$, where N is the number of (—CH=CH—) bonds. Photoluminescence data confirmed this; the mean conjugation length obtained from the fitted distribution of n was around $\langle n \rangle = 8.2$ at 80% *trans*-$(CH)_x$. Applying Hückel theory to this model resulted in good agreement with the experimental photoluminescence data. A value of $\beta_0 = 1.08$ eV was calculated for the interaction energy between adjacent π orbitals in solid-state polyacetylene. We calculate from this value of β_0 that the observed π-π^* energy of 0.45 eV for neutral solitons corresponds to just $n = 7$. Further thermal treatment of polyacetylene apparently resulted in only modest increases in the mean conjugation lengths of the segments. $\langle n \rangle$ in undoped "all-*trans*" polyacetylene was probably less than 13. The picture of polyacetylene that emerged from this study is consistent with a large variety of experimental evidence, and predicts that macroscopic conductivity in polyacetylene depends as much on crosslinking and the resulting enhanced interchain interactions as it does on the extent of conjugation along a single chain.

ACKNOWLEDGMENTS

The authors wish to acknowledge Michael Arndt for building the photoluminescence spectrometer, John Gehlen for assisting with Hückel calculations, and Andrew Streitwieser, Jr., for helpful discussions. Funding was provided in part by the National Science Foundation (Grant No. DMR-8719302).

[1] *Chemistry, Physics, and Material Science of Polyacetylene,* edited by J. C. W. Chien (Academic, New York, 1984); *Handbook of Conducting Polymers,* edited by Terje Skotheim (Dekker, New York, 1986).

[2] H. Shirakawa, T. Ito, and S. Ikeda, Polymer J. **4**, 460 (1973); T. Yamabe, K. Tanaka, H. Teramae, K. Fukui, A. Imamura, H. Shirakawa, and S. Ikeda, Solid State Commun. **29**, 329 (1979).

[3] J. L. Bredas, R. Sibley, D. S. Boudreaux, and R. R. Chance, J. Am. Chem. Soc. **105**, 6555 (1983); A. Szabo, J. Langlet, and J. P. Malrieu, Chem. Phys. **13**, 173 (1976).

[4] E. A. Imhoff, D. B. Fitchen, and R. E. Stahlbush, Solid State Commun. **44**, 329 (1982); K. Yoshino, S. Hayashi, T. Sakai, Y. Inuishi, H. Kato, and Y. Watanabe, Jpn. J. Appl. Phys. **21**, 1653 (1982); K. Yoshino, S. Hayashi, Y. Inuishi, K. Hattori, T. Hyodo, and Y. Watanabe, Solid State Commun. **49**, 1067 (1984).

[5] T. Ito, H. Shirakawa, and S. Ikeda, J. Polym. Sci. Polym. Chem. Ed. **12**, 11 (1974).

[6] M. G. Voronkov, V. B. Pukhnarevich, S. P. Sushchinskaya, V. Z. Annenkova, V. M. Annenkova, and N. J. Andreeva, J. Polym. Sci. Polym. Chem. Ed. **18**, 53 (1980); T. Masuda and T. Higashimura, Acc. Chem. Res. **17**, 51 (1984).

[7] S. Zhiquan, Y. Mujie, S. Mingxiao, and C. Yipling, J. Polym. Sci. Polym. Lett. Ed. **20**, 411 (1982).

[8] G. L. Baker, J. A. Shelburne, and F. S. Bates, J. Am. Chem. Soc. **108**, 7377 (1986).

[9] L. S. Lichtmann, E. A. Imhoff, A. Sarahangi, and D. B. Fitchen, J. Chem. Phys. **81**, 168 (1984); E. Ehrenfreund, Z. Vardeny, O. Brafman, and B. Horovitz, Phys. Rev. B **36**, 1535 (1987).

[10] T. Yamabe, K. Akagi, K. Ohzeki, K. Fukui, and H. Shirakawa, J. Phys. Chem. Solids **43**, 577 (1982).

[11] L Lauchlan, S. Etemad, T.-C. Chung, A. J. Heeger, and A. G. MacDiarmid, Phys. Rev. B **24**, 3701 (1981).

[12] J. F. Rabek, *Mechanisms of Photophysical Processes and Photochemical Reactions in Polymers* (Wiley, New York, 1987), pp. 33–129.

[13] G. Wegner, Angew. Chem. Int. Ed. Engl. **20**, 361 (1981).

[14] G. Zannoni and G. Zerbi, Chem. Phys. Lett. **97**, 147 (1983); A. Bolognesi, M. Catellani, S. Destri, G. Morelli, and M. Zocchi, Makromol. Chem. Rapid Commun. **4**, 403 (1983).

[15] A. Brillante, K. Reimann, and K. Syassen, Chem. Phys. Lett. **151**, 243 (1988); A. Brillante, M. Hanfland, and K. Syassen, *ibid.* **119**, 42 (1985); R. G. Della Valle and A. Brillante, Chem. Phys. **116**, 141 (1987).

[16] K. Knoll and R. R. Schrock, J. Am. Chem. Soc. **111**, 7989 (1989).

[17] T. Ito, H. Shirakawa, and S. Ikeda, J. Polym. Sci. Polym. Chem. Ed. **13**, 1943 (1975); A. Montaner, M. Galtier, C. Benoit, and M. Aldissi, Solid State Commun. **39**, 99 (1981).

[18] A. Streitwieser, Jr., *Molecular Orbital Theory for Organic Chemists* (Wiley, New York, 1961), pp. 202–236.

[19] R. S. Mulliken, C. A. Rieke, and W. G. Brown, J. Am. Chem. Soc. **63**, 41 (1941).

[20] *Molecular Orbital Theory for Organic Chemists* (Ref. 18), p. 104.

[21] C. S. Yannoni and T. C. Clarke, Phys. Rev. Lett. **51**, 1191 1983); C. R. Fincher, C. E. Chen, A. J. Heeger, A. G. MacDiarmid, and J. B. Hastings, *ibid.* **48**, 100 (1982); A. Karpfen and J. Petkov, Theor. Chim. Acta **53**, 65 (1979).

[22] G. B. Blanchet, C. R. Fincher, and A. J. Heeger, Phys. Rev. Lett. **50**, 1938 (1983); L. Rothberg, T. M. Jedju, P. D Townsend, S. Etemad, and G. L. Baker, *ibid.* **65**, 100 (1990).

[23] T. A. Albright, J. K. Burdett, and M. H. Whangbo, *Orbital Interactions in Chemistry* (Wiley, New York, 1985), pp. 211 and 212.

[24] D. S. Boudreaux, R. R. Chance, J. L. Bredas, and R. Sibley, Phys. Rev. B **28**, 6927 (1983); H. Thomann, L. R. Dalton, Y. Tomkiewicz, N. S. Shiren, and T. C. Clarke, Phys. Rev. Lett. **50**, 533 (1983).

[25] T. Forster, Ann. Phys. **2**, 55 (1948); Z. Electrochem. **64**, 157 (1960).

[26] J. B. Birks, D. J. Dyson, and I. H. Munro, Proc. R. Soc. London Ser. A **275**, 575 (1963); J. B. Birks, D. J. Dyson, and T. A. King, *ibid.* **277**, 270 (1964); R. B. Cundall and L. C. Pereira, Chem. Phys. Lett. **18**, 371 (1973).

[27] C. V. Shank, R. Yen, R. L. Fork, J. Orenstein, and G. L. Baker, Phys. Rev. Lett. **49**, 1660 (1982); C. V. Shank, R. Yen, J. Orenstein, and G. L. Baker, Phys. Rev. B **28**, 6095 (1983); J. R. Andrews, T. E. Orlowski, H. Gibson, M. L. Slade, W. Knox, and B. Wittsmershaus, *ibid.* **27**, 6545 (1983).

[28] D. L. Dexter, J. Chem. Phys. **21**, 836 (1953); V. L. Ermolaev, Usp. Fiz. Nauk. **80**, 3 (1963) [Sov. Phys.—Usp. **80**, 333 (1963)].

[29] J. C. W. Chien, F. E. Karasz, and G. E. Wnek, Nature **285**, 390 (1980).